

# Dendritic Spikes in Apical Dendrites of Neocortical Layer 2/3 Pyramidal Neurons

Matthew Evan Larkum, Jack Waters, Bert Sakmann, and Fritjof Helmchen

Abteilung Zellphysiologie, Max-Planck-Institut für Medizinische Forschung, D-69120 Heidelberg, Germany

Layer 2/3 (L2/3) pyramidal neurons are the most abundant cells of the neocortex. Despite their key position in the cortical microcircuit, synaptic integration in dendrites of L2/3 neurons is far less understood than in L5 pyramidal cell dendrites, mainly because of the difficulties in obtaining electrical recordings from thin dendrites. Here we directly measured passive and active properties of the apical dendrites of L2/3 neurons in rat brain slices using dual dendritic–somatic patch-clamp recordings and calcium imaging. Unlike L5 cells, L2/3 dendrites displayed little sag in response to long current pulses, which suggests a low density of  $I_h$  in the dendrites and soma. This was also consistent with a slight increase in input resistance with distance from the soma. Brief current injections into the apical dendrite evoked relatively short (half-width 2–4 ms) dendritic spikes that were isolated from the soma for near-threshold currents at sites beyond the middle of the apical dendrite. Regenerative dendritic potentials and large concomitant calcium transients were also elicited by trains of somatic action potentials (APs) above a critical frequency (130 Hz), which was slightly higher than in L5 neurons. Initiation of dendritic spikes was facilitated by backpropagating somatic APs and could cause an additional AP at the soma. As in L5 neurons, we found that distal dendritic calcium transients are sensitive to a long-lasting block by GABAergic inhibition. We conclude that L2/3 pyramidal neurons can generate dendritic spikes, sharing with L5 pyramidal neurons fundamental properties of dendritic excitability and control by inhibition.

**Key words:** neocortex; synaptic; integration; action potential; calcium; coincidence detection

## Introduction

Pyramidal neurons in layer 2/3 (L2/3) constitute the majority of cells in the neocortex (Zilles, 1990). They are thought to be fundamental for cortical tasks such as feature selection and perceptual grouping (Grossberg and Raizada, 2000; Binzegger et al., 2004). Their morphology is similar to L5 pyramidal neurons, but the apical dendrite is thinner and shorter (Larkman et al., 1992). The differences in dendritic length and diameter have implications for their electrical compactness and integrative properties (Larkman et al., 1992; Zador et al., 1995). L5 pyramidal neurons have a rich assembly of dendritic conductances and correspondingly rich input–output capabilities. It has been assumed that L2/3 pyramidal neurons possess a composition of dendritic conductances similar to other pyramidal neurons (Wang, 1999; Traub et al., 2003). However, little is known about the regenerative properties of the apical dendrites of L2/3 pyramidal neurons except that they sustain active backpropagation of action poten-

tials (APs) supported by dendritic  $\text{Na}^+$  channels (Waters et al., 2003; Waters and Helmchen, 2004) and have a concomitant influx of calcium ions (Svoboda et al., 1999).

Studies of dendritic excitation have focused on the large thick-tufted L5 neurons mainly for technical reasons. Although direct patch-clamp recordings from the apical dendrite of L5 neurons have become a routine technique (Gulledge et al., 2005), similar experiments on L2/3 neurons are more difficult because of their thinner dendrites. Here, we have overcome this difficulty by combining infrared differential interference contrast (IR-DIC) with fluorescence microscopy for guidance of patch pipettes. This approach enabled us, for the first time to our knowledge, to obtain simultaneous recordings from the somata and apical dendrites of L2/3 neurons in brain slices of rat somatosensory cortex. These dual recordings permitted us to study the subthreshold attenuation of synaptic potentials generated in the tuft as they spread toward the soma as well as the ability of the apical dendrite to actively participate in suprathreshold dendritic signaling.

L2/3 neurons receive their input predominantly from other L2/3 pyramidal neurons and L4 spiny stellate neurons (Lübke et al., 2003; Binzegger et al., 2004). These inputs project almost exclusively to the basal and apical oblique dendrites. Inputs to the apical tuft are thought to be feedback connections from higher cortical areas and nonspecific thalamic nuclei (Felleman and Van Essen, 1991). These connections show synaptic depression (Walcott and Langdon, 2001), can elicit APs, and can be potentiated by theta-burst stimulation (Walcott and Langdon, 2002). In L5 neurons, distal inputs can induce AP bursts via dendritic  $\text{Ca}^{2+}$  spikes

Received April 17, 2007; revised June 24, 2007; accepted June 26, 2007.

This work was supported by a Marie Curie individual fellowship from the European Community (J.W.) (Contract Number QLGA-CT-2001-50999). We thank Paul Rhodes for helpful discussions and comments on this manuscript and Marlies Kaiser for expert technical assistance.

Correspondence should be addressed to Matthew Larkum at his present address: Institute of Physiology, University of Bern, Bühlpplatz 5, CH-3012 Bern, Switzerland. E-mail: larkum@pyl.unibe.ch.

J. Waters' present address: Department of Physiology, Feinberg School of Medicine, Northwestern University, 303 East Chicago Avenue, Chicago, IL 60611.

F. Helmchen's present address: Department of Neurophysiology, Brain Research Institute, University of Zurich, Winterthurerstrasse 190, CH-8057 Zurich, Switzerland.

DOI:10.1523/JNEUROSCI.1717-07.2007

Copyright © 2007 Society for Neuroscience 0270-6474/07/278999-10\$15.00/0

(Connors and Gutnick, 1990; Amitai et al., 1993; Kim and Connors, 1993; Schiller et al., 1997; Larkum et al., 1999b, 2004; Larkum and Zhu, 2002). We were therefore particularly interested to determine whether spikes can be initiated in L2/3 distal apical dendrites. Although burst firing has been observed in L2/3 pyramidal neurons *in vivo* (Gray and McCormick, 1996), it is unclear whether AP bursting in L2/3 pyramids can be generated by distal dendritic input. Here, we find that L2/3 neurons are capable of generating dendritic spikes and associated calcium influx but not bursts consisting of three or more APs.

## Materials and Methods

**Slice preparation.** Experiments were performed in somatosensory neocortical slices from postnatal day 27–43 ( $n = 46$ ) Wistar rats using procedures described previously (Waters et al., 2003). Rats were deeply anesthetized with halothane and decapitated. The brain was quickly removed into cold ( $0$ – $4^{\circ}\text{C}$ ), oxygenated physiological solution containing the following (in mM): 125 NaCl, 2.5 KCl, 1.25  $\text{NaH}_2\text{PO}_4$ , 25  $\text{NaHCO}_3$ , 1  $\text{MgCl}_2$ , 25 glucose, and 2  $\text{CaCl}_2$ , pH 7.4. Parasagittal slices, 300  $\mu\text{m}$  thick, were cut from the tissue block with a vibratome and kept at  $37^{\circ}\text{C}$  for 30 min and then at room temperature until use.

**Electrophysiology.** All experiments were performed at  $34.0 \pm 0.5^{\circ}\text{C}$ . Single L2/3 pyramidal neurons were identified using IR-DIC optics. Somatic ( $5$ – $10\ \text{M}\Omega$ ) and dendritic ( $\sim 20\ \text{M}\Omega$ ) recording pipettes were filled with intracellular solution containing the following: 105 mM K-gluconate, 10 mM HEPES, 2 mM  $\text{MgCl}_2$ , 2 mM MgATP, 2 mM  $\text{Na}_2\text{ATP}$ , 0.3 mM GTP, 30 mM KCl, and 0.2% biocytin, pH 7.3. The intracellular solution also contained 10  $\mu\text{M}$  Alexa 468 (Invitrogen, Carlsbad, CA), which was used to visualize the dendritic tree by fluorescence microscopy after establishing a whole-cell recording at the cell body. Here, an overlaid, static fluorescence/DIC image was compared with a live DIC image for positioning the pipette precisely onto the dendrite of the somatically patch-clamped neuron. Whole-cell recordings were made with Axoclamp-2B amplifiers (Molecular Devices, Palo Alto, CA). Synaptic stimulation was made via a glass pipette placed in the superficial half of L1, 100–200  $\mu\text{m}$  from the axis of the apical dendrite. In some experiments, 2.5  $\mu\text{M}$  bicuculline (Sigma, St. Louis, MO) and 1  $\mu\text{M}$  (2S)-3-[(1S)-1-(3,4-dichlorophenyl)ethyl]amino-2-hydroxypropyl(phenylmethyl)phosphonic acid (CGP 55845; Tocris Bioscience, Ellisville, MO) were added to the extracellular solution. After recordings, slices were fixed and stained as described previously (Schiller et al., 1997) for later reconstruction.

**Calcium imaging.** For optical recording of dendritic  $\text{Ca}^{2+}$  transients, we combined dual whole-cell recording with  $\text{Ca}^{2+}$  imaging. Neurons were loaded with a fluorescent  $\text{Ca}^{2+}$  indicator [100  $\mu\text{M}$  Oregon Green 488 BAPTA-1 (OGB-1); Invitrogen], which was added to the internal solution. Fluorescence changes were detected using a  $512 \times 512$  back-illuminated frame-transfer CCD camera (PXL or MicroMax; Roper, Tucson, AZ). Images were binned at  $5 \times 5$  or  $10 \times 10$  and acquired at a frame rate of  $\sim 40$  Hz. For measurements of the relative fluorescence changes from baseline ( $\Delta F/F$ ), two methods were used. First, regions of

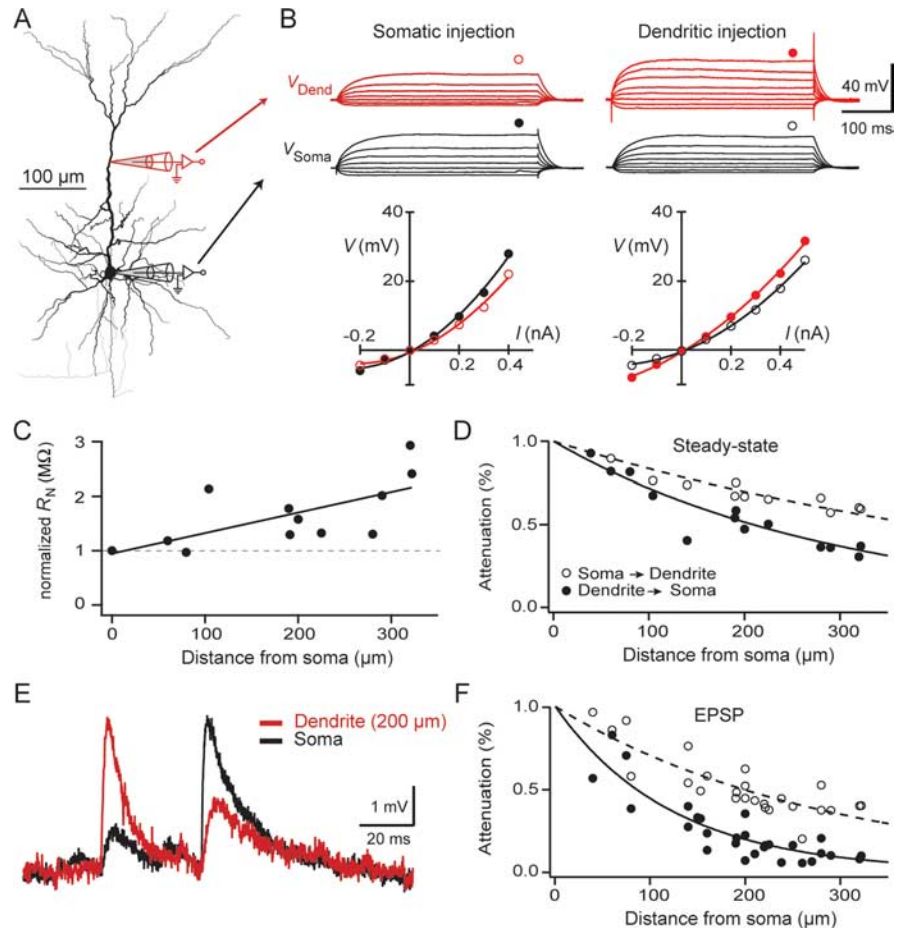


**Figure 1.** Subthreshold properties of L2/3 pyramidal neurons. **A**, Reconstruction of an L2/3 pyramidal neuron filled with biocytin during the experiment. Cell body was at 430  $\mu\text{m}$  from the pia. The locations of the two recording pipettes are shown diagrammatically. The dendritic patch electrode (red) was 190  $\mu\text{m}$  from the soma. **B**, Simultaneous recording of somatic voltage (black traces) and dendritic voltage (red traces) during either somatic (left) or dendritic (right) injections of 400-ms-long current steps. Resting membrane potential was  $-81.4$  and  $-80$  mV at soma and dendrite, respectively. The steady-state  $V$ - $I$  relationships at soma and dendrite are shown below for both somatic and dendritic current injection. Note prominent anomalous rectification (Waters and Helmchen, 2006). **C**, Input resistance at resting membrane potential as a function of distance from the soma. Values are normalized to the input resistance at the soma for each cell. A straight line fit to the data shows an increase of 37% per 100  $\mu\text{m}$ . **D**, Steady-state voltage attenuation along the apical dendrite for current pulses injected into the dendrite (filled circles) and the soma (open circles). Both somatopetal and somatofugal attenuation were fitted with exponential curves. **E**, Example of two spontaneous EPSPs recorded at the soma (black trace) and in the apical dendrite 200  $\mu\text{m}$  from the soma (red trace). **F**, Somatopetal (open circles) and somatofugal (filled circles) attenuation of spontaneous EPSPs as a function of distance along the apical dendrite for 28 different L2/3 neurons.

interest (ROIs) in the dendrites were selected off-line at different locations from the soma. For each ROI, two background ROIs of the same dimensions were placed nearby over a region not including the cell. These were averaged and subtracted from the total fluorescence before calculating  $\Delta F/F$  (Helmchen, 2005). A second method of determining  $\Delta F/F$  was based on a spatial profile, which we determined off-line by placing a line along the dendrite (and an adjacent line for background subtraction  $\sim 10$ – $20\ \mu\text{m}$  from the profile line).  $\Delta F/F$  values were calculated by dividing pixel-by-pixel the fluorescence values in each frame by the average of the prestimulus frames.

Pooled results are reported as mean  $\pm$  SD except when noted. Regression statistics were performed using the program GBStat (Dynamic Microsystems, Silver Spring, MD).

## Results

### Dual somatic–dendritic recordings from L2/3 pyramidal neurons

We examined L2/3 pyramidal neurons of the somatosensory cortex in 4- to 6-week-old rats using dual somatic and dendritic

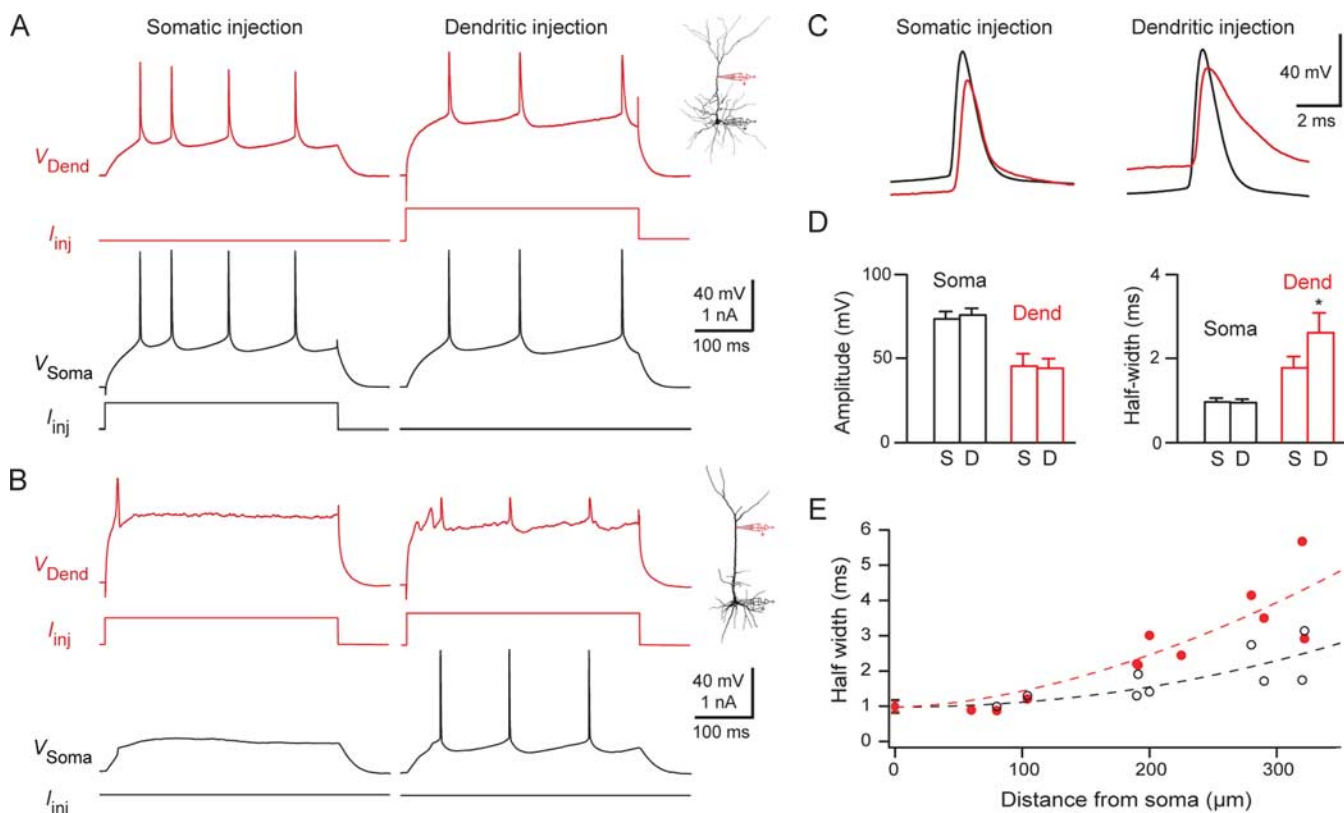


**Figure 2.** Suprathreshold properties of L2/3 pyramidal neurons. **A**, Simultaneous recording of somatic (black traces) and dendritic (red traces) membrane potential during suprathreshold current injections into either soma (left) or dendrite (right). Same cell as shown in Figure 1A. Current thresholds for eliciting APs were 0.5 and 0.6 nA, respectively. Resting membrane potential was  $-81.4$  and  $-80$  mV at soma and dendrite, respectively. **B**, Responses to dendritic current injection in another cell. Left, Injection of 0.5 nA resulted in an isolated dendritic spike. Right, A slightly greater current injection (0.6 nA) caused a second dendritic spike before a series of backpropagating somatic APs was elicited. Resting membrane potential was  $-72.5$  and  $-69.5$  mV at soma and dendrite, respectively. Somatic depth was  $450 \mu\text{m}$ . The dendritic recording pipette was located  $270 \mu\text{m}$  from the soma. **C**, Expanded view of the first APs of each train shown in **A**. Dendritic voltage traces are shown in red. Note that, in both cases, the AP occurred first at the soma. With dendritic current injection, the dendritic AP was longer compared with somatic injection (half-width of 2.1 vs 1.2 ms). Resting membrane potential was  $-81$  and  $-80$  mV at soma and dendrite, respectively. **D**, Analysis of amplitude from threshold (left) and half-width (right) of somatic APs (black bars) and dendritic APs (red bars) for both somatic (S) and dendritic (D) current injections. Dendritic APs were significantly broader during dendritic current injection ( $p < 0.05$ ). **E**, Dependence on the AP half-width on distance from soma for somatic (black open circles) and dendritic (red filled circles) current injections.

whole-cell recordings *in vitro*. The mean depth of cell somata below the pia was  $421 \pm 58 \mu\text{m}$  (range of  $276$ – $505 \mu\text{m}$ ;  $n = 36$ ). To determine basic cellular properties, we injected 400-ms-long current pulses at either the dendritic or the somatic electrode. We first analyzed subthreshold voltage deflections (Fig. 1). All cells displayed a steady-state voltage–current ( $V$ – $I$ ) relationship showing anomalous rectification (Fig. 1B). Mean input resistance at resting membrane potential was  $30.6 \pm 10.7 \text{ M}\Omega$  ( $n = 9$ ) at the soma and increased with distance from the soma (Fig. 1C) (mean dendritic input resistance,  $42.1 \pm 11.9 \text{ M}\Omega$  for distances between  $60$  and  $322 \mu\text{m}$  from the soma;  $n = 10$ ). Membrane time constants were  $8.0 \pm 1.3$  ms for the soma and  $8.0 \pm 1.8$  ms for dendritic sites. Rectification was quantified using a quadratic fit to the  $I$ – $V$  curves (Waters and Helmchen, 2006), yielding mean rectification coefficients of  $37.1 \pm 23.1$  and  $26.1 \pm 14.5 \text{ M}\Omega/\text{nA}$  for soma and dendrite, respectively.

In contrast to L5 pyramidal neurons, which show prominent sag in the voltage response to long current injections (30–40% in tuft dendrites in 28-d-old rats) (Zhu, 2000), L2/3 neurons displayed little sag either at the soma or in the dendrite ( $1.4 \pm 2.5$  and  $3.2 \pm 4\%$ , respectively; full dendritic range from  $60$  to  $322 \mu\text{m}$ ). This indicates that less hyperpolarization-activated ( $I_h$ ) current is present in the dendrites of L2/3 neurons than in L5 pyramidal neurons.

We next examined bidirectional voltage attenuation between

the soma and dendrite. Steady-state attenuation was determined by analyzing voltage deflections in response to small hyperpolarizing currents and fitting the distance dependence of amplitude attenuation with an exponential curve (Fig. 1D). In the somatopetal direction (dendrite to soma), the space constant  $\lambda_{\text{Fit}}$  was  $302 \mu\text{m}$ , and, in the somatofugal direction (soma to dendrite),  $\lambda_{\text{Fit}}$  was  $556 \mu\text{m}$ . We also estimated the attenuation of spontaneous EPSPs. Although it was not possible to determine the exact origin of EPSPs from the dual-site recordings, we could in many cases identify the direction of propagation based on the order of onset at the two electrodes and the slopes of the rising phases of the EPSPs. In the example shown in Figure 1E, the first EPSP propagated somatopetally and was attenuated to 25% of its original amplitude, whereas the second, somatofugally propagating EPSP was attenuated to 46% at the dendritic recording site. In 28 neurons, we found a mean somatopetal EPSP attenuation constant ( $\lambda_{\text{EPSP}}$ ) of  $122 \mu\text{m}$  and a mean somatofugal  $\lambda_{\text{EPSP}}$  of  $283 \mu\text{m}$  (Fig. 1F). Thus, as expected for transient membrane changes (Agmon-Snir and Segev, 1993), EPSPs were more strongly attenuated than steady-state membrane changes and spontaneous EPSPs were attenuated differently depending on the direction of propagation (Zador et al., 1995). On average, a distal EPSP was attenuated to approximately one-third its original amplitude over  $120 \mu\text{m}$ , which is approximately one-quarter of the total apical dendritic length for L2/3 pyramidal neurons.

Suprathreshold current injections at both soma and dendrite caused regularly spiking trains of APs showing spike frequency adaptation in all cells (Fig. 2A). With long current pulses, APs in nearly all cases initiated at the soma regardless of the site of current injection (Fig. 2A). Only in 3 of 36 cells was an isolated dendritic spike (i.e., no somatic AP) elicited at threshold current injection to the dendrite (Fig. 2B). The amplitude of the dendritic backpropagating APs (bAPs) showed decremental attenuation with distance from the soma as reported previously (Waters et al., 2003). Dendritic bAP amplitudes were similar regardless of the site of current injection (Fig. 2C,D) (amplitude from threshold,  $46.3 \pm 19.6$  and  $45.0 \pm 16.3$  mV for somatic and dendritic injection, respectively;  $p > 0.25$ ). Backpropagating APs were, however, significantly broader in the dendrite when long current pulses were injected at the dendritic site (Fig. 2C,D) (half-width,  $1.8 \pm 0.7$  and  $2.6 \pm 1.5$  ms for somatic and dendritic injection, respectively;  $p < 0.05$ , paired *t* test). This suggests that additional dendritic voltage-activated channels are activated during dendritic compared with somatic stimulation. This is consistent with an increased  $\text{Ca}^{2+}$  influx during sustained depolarization of the dendrite (Waters and Helmchen, 2004).

With further increased current injections the interspike intervals (ISIs) of the AP trains were reduced. The ISI of the first two APs became disproportionately faster, whereas all other ISIs in the train remained more or less regular. Hence, large current injections produced an initial doublet of spikes followed by a train of evenly spaced APs (supplemental Fig. 1, available at [www.jneurosci.org](http://www.jneurosci.org) as supplemental material).

### Critical frequency for dendritic regenerative potentials

Because only a small fraction of cells produced dendritic spikes during long current injections, we asked whether trains of APs summate in the distal dendrite to induce additional dendritic conductances, as in L5 pyramidal neurons (Larkum et al., 1999a). Using somatic–dendritic dual recordings, we examined the amplitudes of APs in the dendrite during low-frequency (10–20 Hz) trains of APs produced by trains of short current pulses injected at the soma (Fig. 3). We found that the AP amplitude in the dendrite decreased only slightly during low-frequency trains of 10 APs (~20% accommodation at 250  $\mu\text{m}$  from the soma) (Fig. 3A). Pooled results for low-frequency trains (10–20 Hz) in 25 neurons confirm that there was very little attenuation even for the most distal recordings (Fig. 3B). This contrasts with results from neocortical L5 and hippocampal CA1 pyramidal neurons, which show pronounced activity-dependent attenuation of AP backpropagation in the apical dendrite (Spruston et al., 1995; Larkum et al., 2001).

In contrast, during higher-frequency AP trains (50 and 160 Hz), the dendritic amplitude of the last APs in the train increased in a frequency-dependent manner (Fig. 4A,B). The change in AP

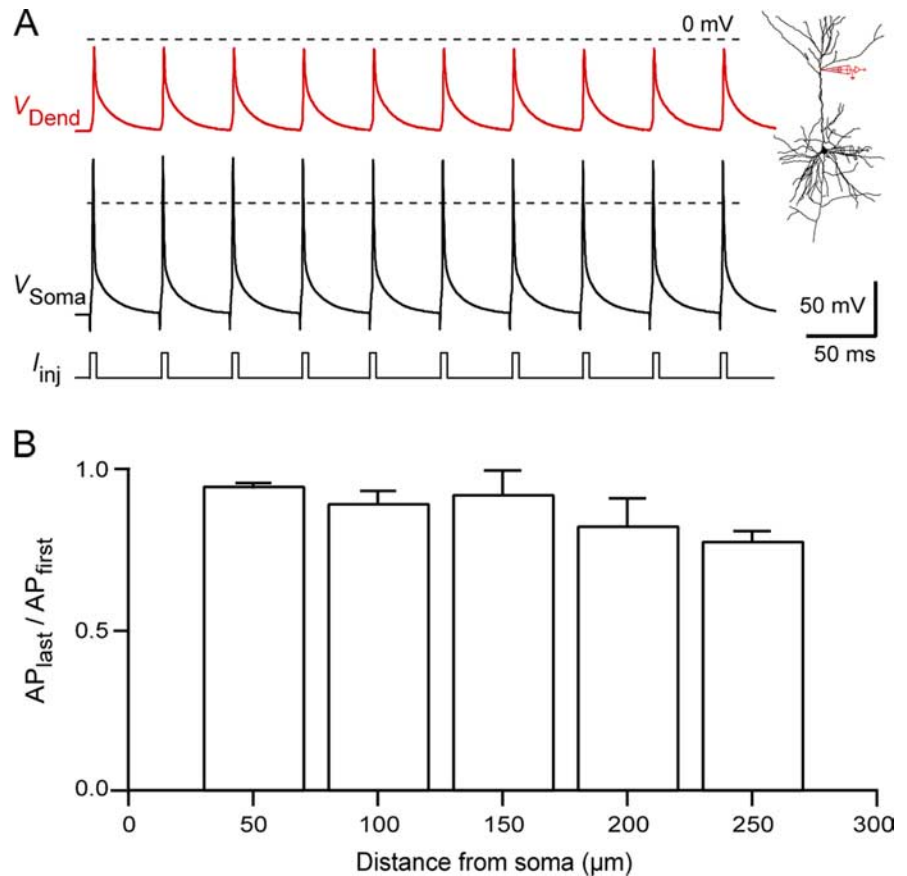


**Figure 3.** Little inactivation of bAPs during AP trains in L2/3 neurons. **A**, Dual recording from an L2/3 pyramidal neuron. Somatic (black trace) and dendritic (red trace) membrane potential in response to a 10 Hz train of 2 ms current pulses delivered at the soma to produce a train of 10 APs. Note that there is little attenuation of the dendritic AP amplitude. The reconstructed L2/3 cell is shown on the right. The soma was 435  $\mu\text{m}$  from the pia. The dendritic pipette was located 227  $\mu\text{m}$  from the soma. **B**, The average ratio of the dendritic amplitude of the last AP to the first AP of similar trains in 25 neurons, shown as a function of distance from soma (bin width, 50  $\mu\text{m}$ ). Only a small tendency toward increased attenuation with distance from the soma is apparent.

amplitude occurred over a narrow “critical” frequency (CF) range, above which an additional regenerative component was recruited, as in L5 neurons (Larkum et al., 1999a). The difference in dendritic AP amplitude was also reflected at the soma by an increase in the afterdepolarizing potential (ADP) of ~1.5 mV (Fig. 4B). Although small, the somatic effect occurred consistently from trial to trial and from cell to cell. In addition, amplified dendritic APs were associated with large dendritic calcium influx (Fig. 4C).

The CF was not significantly different whether it was determined at the peak of the last dendritic AP or at a later time point from the change in the somatic afterpotential (Fig. 4D) ( $117 \pm 13$  and  $118 \pm 13$  Hz for dendritic and somatic traces, respectively;  $p > 0.5$ , paired *t* test). Similar CF values were also obtained from dendritic calcium signals and somatic ADPs measured in a separate set of experiments (Fig. 4E) ( $121 \pm 22$  and  $126 \pm 23$  Hz, respectively;  $p > 0.05$ ). Finally, because there was no significant difference between the CFs measured at the dendrite and the soma, we evaluated the CFs in many neurons with only somatic recordings. The average CF for 68 L2/3 pyramidal neurons using this method was  $128 \pm 21$  Hz (Fig. 4F), and the average change in ADP amplitude was  $2.9 \pm 1.9$  mV (Fig. 4G). We conclude that amplified dendritic potentials with concomitant large calcium influx are generated by high-frequency somatic stimulation, con-

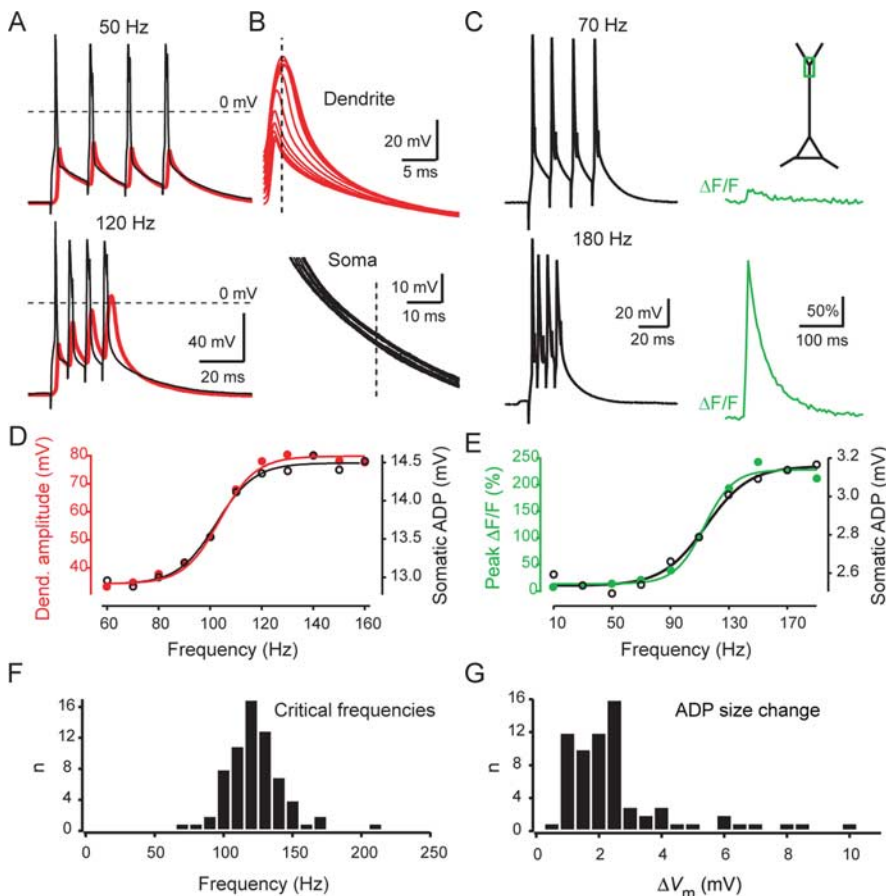


**Figure 4.** Critical frequency for dendritic electrogenesis. **A**, Dual recording from an L2/3 pyramidal neuron. Somatic (black trace) and dendritic (red trace) membrane potential in response to trains of APs at 50 Hz (top) and 120 Hz (bottom) evoked by brief somatic current injections. The resting membrane potential at the soma and the dendrite was  $-73$  and  $-75$  mV, respectively. The soma was  $450 \mu\text{m}$  from the pia. The dendritic pipette was located  $270 \mu\text{m}$  from the soma. **B**, Overlay of the last AP during trains of four APs at different frequencies from 50 to 160 Hz for dendritic (top) and somatic (bottom) recording. The peak amplitude of the last AP recorded at the dendrite increased in a nonlinear manner. This was also reflected in the dendritic and somatic traces at later times (e.g., at the time point indicated by dashed line). **C**, Simultaneous somatic membrane potential recording (left) and dendritic calcium imaging near the principal bifurcation (right) in another L2/3 neuron. Trains of four APs at 70 Hz (top) and 180 Hz (bottom) were evoked by brief somatic current injections. Note the large calcium transient evoked at high frequency. **D**, Peak amplitudes of dendritic APs (red filled circles) and amplitudes of the somatic ADP (black open circles) as a function of frequency, showing a sharp increase at  $\sim 90$ – $120$  Hz. The CF was determined as the turning point of a sigmoidal fit. **E**, Peak amplitudes of dendritic calcium transients (green filled circles) and amplitudes of the somatic ADP (black open circles) as a function of frequency, fitted with sigmoidal curves. **F**, Distribution of CFs (taken as half-maximal frequencies of the sigmoidal fits to ADPs as shown in **D** and **E**) for 68 L2/3 neurons. **G**, Distribution of the changes in ADP size (taken as the amplitude of the sigmoidal fit) for the same neurons as in **F**.

sistent with the supralinear calcium influx into L2/3 dendrites during bursts of APs reported previously (Waters et al., 2003).

#### Dendritic spikes evoked by simulated EPSPs

In L5 pyramidal neurons, short current injections are more likely to elicit dendritic spikes than longer injections (Larkum et al., 2001). Because long current injections rarely evoked dendritic spikes at threshold, we investigated whether EPSP-like waveforms would evoke dendritic spikes in L2/3 neurons (Fig. 5). We injected a double-exponential current waveform with rising and falling time constants of 2 and 8 ms, respectively, resulting in a waveform with  $\sim 3.5$  ms time-to-peak. When injected into the dendrite, this waveform elicited EPSP-like traces with a time course at the soma similar to a typical EPSP evoked by extracellular stimulation in L1 (half-widths at the soma  $15.4 \pm 0.5$  and  $14.9 \pm 0.8$  ms, respectively;  $n = 14$  and  $n = 13$ ;  $p > 0.6$ ). We then

increased the amplitude of the simulated EPSP until it evoked a dendritic spike (Fig. 5A). The threshold for eliciting a dendritic spike was  $1.8 \pm 0.6$  nA ( $n = 21$ ). In some cases, the dendritic spike was coupled with a somatic AP (Fig. 5B). Our criterion for a dendritic spike was either an isolated spike at the dendritic electrode (Fig. 5A, Isolated) or a spike that arose at the dendritic electrode before the somatic AP (Fig. 5B, Coupled). To quantify the regenerative dendritic component, we subtracted the “subthreshold” component (estimated by extrapolation from voltage responses to the previous two current steps) from the dendritic spike at threshold (Fig. 5A, middle traces). Average values of the amplitude and half-width of the additional potential ( $V_{\text{Diff}}$ ) were  $20.7 \pm 7.9$  mV and  $2.6 \pm 0.9$  ms, respectively ( $n = 11$ ). In four cells, we could analyze the extra somatic depolarization caused by the dendritic spike, which was  $12 \pm 3\%$  of the dendritic amplitude ( $2.0 \pm 1.1$  vs  $16.0 \pm 5.0$  mV). The amplitude of the calculated dendritic regenerative potential was not dependent on the distance of the dendritic electrode from the soma (correlation coefficient of 0.1;  $p > 0.05$ ), but the width of the dendritic potential was correlated with distance (correlation coefficient of 0.56;  $p < 0.05$ ) (supplemental Fig. 2, available at [www.jneurosci.org](http://www.jneurosci.org) as supplemental material). A small negative component was apparent in the calculated potential after the dendritic spike, suggesting a contribution from  $\text{K}^+$  channels. Isolated or coupled dendritic spikes were also observed in four experiments with synaptic stimulation in layer 1 (supplemental Fig. 3, available at [www.jneurosci.org](http://www.jneurosci.org) as supplemental material).

We further characterized the coupling of the dendritic spike to the soma by calculating the ratio of the dendritic currents required to reach threshold for eliciting a dendritic spike and a somatic AP, respectively (Fig. 5C).

A ratio of  $< 1$  indicates an isolated dendritic spike at threshold. Ratio of 1 indicates a coupled dendritic spike at threshold. A ratio of  $> 1$  indicates that a somatic spike was evoked at threshold but a coupled dendritic spike could be evoked with increased current injections. The ratio of the threshold currents clearly depended on the distance of the dendritic recording from the soma (Fig. 5C). A regression line fit to the data points crossed the unity line at  $170 \mu\text{m}$ , indicating that dendritic current injection beyond  $170 \mu\text{m}$  from the soma typically results in a dendritic spike at threshold. Because L2/3 neurons have variable length, we also analyzed where an input should occur relative to the length of the dendrite to elicit a dendritic spike at threshold (Fig. 5D). To this end, we marked the positions of the dendritic injection electrodes along a schematic L2/3 pyramidal neuron, normalized to the total distance between soma and pia (Fig. 5D). From this schematic, it is clear that a dendritic spike is likely to result from

current injection into much of the apical dendrite, including more than half of its total length.

In all neurons, it was possible to inject sufficiently large current at the dendritic electrode to evoke a somatic AP. In some cases, it was possible to generate a doublet of APs at the soma, but the current threshold for somatic doublets was always higher than that for a single coupled AP. This contrasts with layer 5 neurons, in which even at threshold a dendritic spike frequently generates a somatic burst of two or more APs (Larkum et al., 1999b; Schwandt and Crill, 1999). Nonetheless, the dendritic component was still complex in L2/3 neurons, involving multiple regenerative components, some of which occurred before the bAP but became mixed with it (Figs. 5B, 6). The half-width of this complex potential waveform in the dendrite was up to 50 ms.

### Backpropagating APs facilitate dendritic spike generation

The threshold for inducing a dendritic spike could be reduced by pairing dendritic current injection with a bAP (Fig. 6). For isolated dendritic spikes, the current threshold was reduced by  $25 \pm 7\%$  when a somatic AP was elicited by a brief current injection 10 ms before the dendritic EPSP-shaped injection (Fig. 6A,C) ( $n = 11$ ). Similarly, pairing a bAP with an EPSP-shaped dendritic waveform reduced the threshold for coupled APs by  $24 \pm 10\%$  (Fig. 6B,C) ( $n = 8$ ). The optimal timing for this facilitatory effect occurred with the dendritic current injection after the somatic current injection by 5–10 ms ( $n = 7$ ; compared with 5 ms in L5 cells) (Larkum et al., 1999b). This facilitatory effect was not dependent on the passive spread of somatic depolarization because it was not observed with current injection just below threshold for a somatic AP (supplemental Fig. 4, available at [www.jneurosci.org](http://www.jneurosci.org) as supplemental material). In some cases, the pairing protocol led to an additional somatic AP at dendritic currents insufficient to cause a somatic spike under control conditions (e.g., for the cell in Fig. 6, a 2 nA waveform injected at the dendrite alone caused an isolated dendritic spike, whereas it was sufficient to cause a second somatic AP when paired with a bAP). This phenomenon is therefore similar to the backpropagation-activated  $\text{Ca}^{2+}$  spike (BAC) firing seen in L5 pyramidal neurons (Larkum et al., 1999b) in that the bAP facilitates a dendritic spike. In L5 neurons, BAC firing typically triggers a burst of three or more somatic APs. Although a doubling of the number of APs in L2/3 pyramidal neurons is possible with simultaneous input to the soma and apical trunk, in contrast with layer 5 neurons, we never observed more than two APs at threshold. This probably results from the briefer duration of dendritic spikes in layer 2/3 neurons, which never caused AP bursting (see above).

As reported previously (Waters et al., 2003), pairing a bAP and

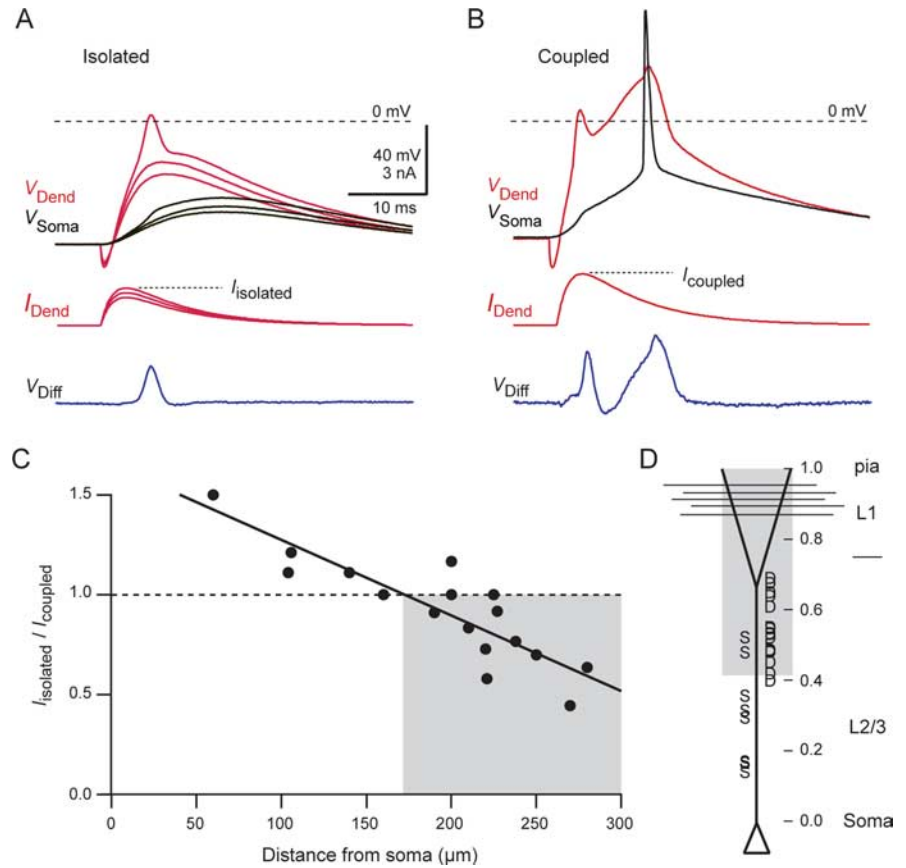


**Figure 5.** Dendritically evoked APs. **A**, EPSP-like current waveform injected into the apical dendrite of an L2/3 pyramidal neuron at  $220 \mu\text{m}$  from the soma. The threshold current  $I_{\text{isolated}}$  needed for evoking an isolated dendritic spike was 1.6 nA (dotted line; middle). Both dendritic (red traces) and somatic (black traces) membrane potential recordings are shown. The regenerative component of the dendritic spike (bottom, blue trace) was calculated by subtracting the predicted nonregenerative component (using the previous subthreshold traces) from the suprathreshold dendritic recording. **B**, In the same neuron, larger dendritic current injection ( $I_{\text{coupled}}$ , 2.2 nA, dotted line, middle trace) resulted in a dendritic spike coupled to a complex potential waveform including an AP at the soma that backpropagated into the dendrite. The regenerative component (bottom, blue trace), calculated in the same manner as **A**, consists of two peaks. **C**, The ratio of  $I_{\text{isolated}}/I_{\text{coupled}}$  as a function of distance from the soma. Ratio values below 1 (dotted line) indicate the experiments in which an isolated dendritic spike could be elicited at threshold (shaded gray area,  $>170 \mu\text{m}$ ). **D**, AP initiation site at threshold dendritic current shown using a schematic diagram of an L2/3 pyramidal neuron with normalized distance measured from the soma relative to the pia. “D” indicates that the AP occurred first in the dendrite (or was an isolated dendritic event). “S” indicates that the AP threshold was reached first at the soma. The gray shaded area indicates the region that is likely to give isolated dendritic spikes with EPSP-like depolarization, calculated from **C**.

an EPSP evoked a large  $\text{Ca}^{2+}$  transient in the distal dendrite ( $115 \pm 61\% \Delta F/F$  compared with  $5 \pm 4\%$  for bAP alone and  $5 \pm 3\%$  for EPSP alone;  $n = 4$ ). This value was not significantly different from the  $\Delta F/F$  value obtained with suprathreshold burst stimulation at the soma of the same cells ( $124 \pm 74\% \Delta F/F$ ;  $p = 0.68$ , paired  $t$  test), indicating that in both cases a regenerative dendritic potential was triggered. In one experiment, we succeeded in measuring the distal  $\text{Ca}^{2+}$  transient evoked by an isolated dendritic spike, demonstrating that a large  $\text{Ca}^{2+}$  influx was associated with the brief dendritic spike in an all-or-none manner (Fig. 6D).

### Inhibitory control of the distal apical dendrite

As in L5 pyramidal neurons (Larkum et al., 1999b), the dendritically evoked distal  $\text{Ca}^{2+}$  influx that accompanied BAC firing could also be elicited with extracellular stimulation of L1 fibers, but only if GABAergic transmission was partially blocked with  $2.5 \mu\text{M}$  bicuculline ( $\text{GABA}_A$ ) and  $1 \mu\text{M}$  CGP 55845 ( $\text{GABA}_B$ ) (Fig. 7). Higher concentrations of bicuculline led to epileptiform discharges in the pyramidal neuron. Figure 7A shows an image of a

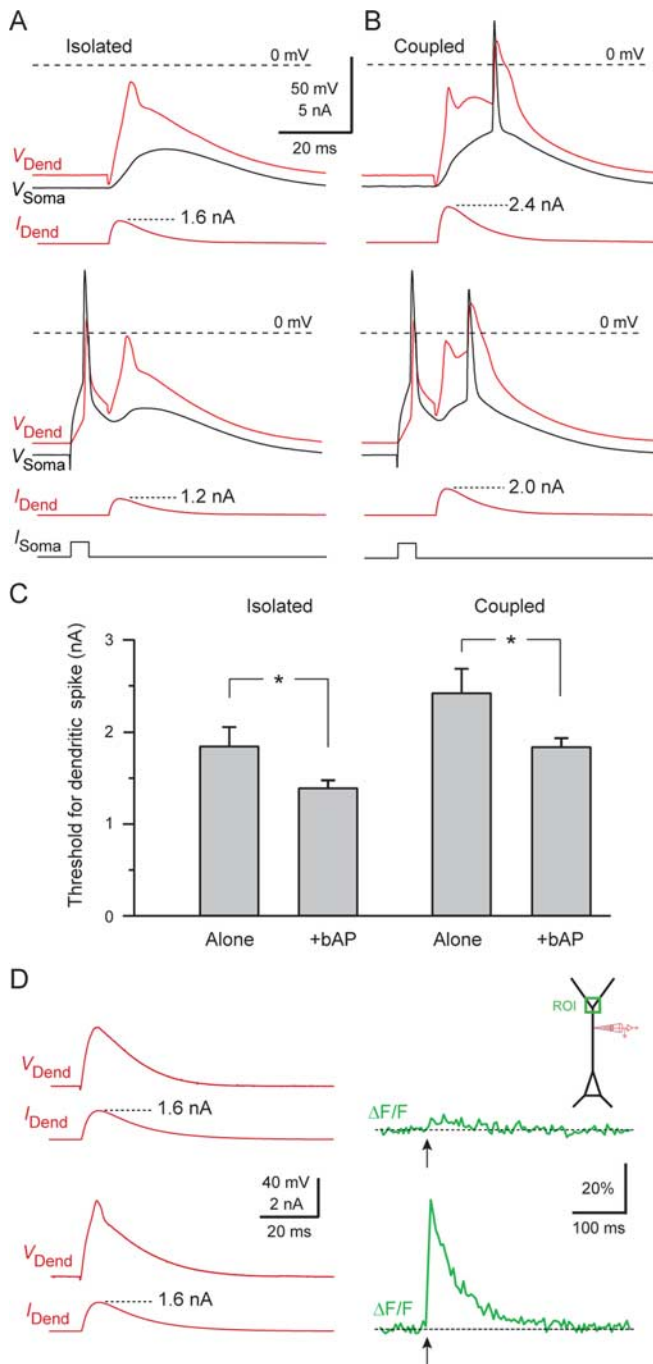


**Figure 6.** Facilitation of dendritic spikes in L2/3 neurons by backpropagating APs. **A**, Example of an L2/3 pyramidal neuron in which a 1.6 nA EPSC-shaped current injection into the dendrite caused an isolated dendritic spike (top). The current threshold for a dendritic spike was reduced to 1.2 nA when a somatically evoked AP preceded the dendritic current injection by 10 ms (bottom). **B**, Example of a coupled dendritic spike in the same L2/3 pyramidal neuron. The threshold current (2.4 nA, top) was reduced to 2.0 nA when a somatically evoked AP preceded the dendritic current injection by 10 ms (bottom). **C**, Average current thresholds necessary to evoke isolated ( $n = 11$  neurons) and coupled ( $n = 8$ ) dendritic spikes with and without a bAP.  $*p < 0.001$ . **D**, Two examples of near-threshold current injection into the apical dendrite, of which one elicited an isolated dendritic spike. Note the large  $\text{Ca}^{2+}$  influx into the distal dendrite associated with the dendritic spike, whereas little  $\text{Ca}^{2+}$  influx occurred when the dendrite remained subthreshold.

biocytin-filled L2/3 neuron indicating the regions that were imaged during the experiment after the cell had been filled with the  $\text{Ca}^{2+}$  indicator OGB-1. White boxes show regions of interest at

different distances along the apical dendrite (115, 260, and 365  $\mu\text{m}$ ). A single bAP caused almost no increase in  $[\text{Ca}^{2+}]_i$  in the distal tuft (Fig. 7B) (Waters et al., 2003), and there was also very little increase with paired distal synaptic input using an extracellular stimulating electrode in L1 (Fig. 7B). However, with antagonists of inhibitory receptors in the perfusate, the  $\Delta[\text{Ca}^{2+}]_i$  along the dendrite increased, and a very large  $\Delta[\text{Ca}^{2+}]_i$  in the tuft region was uncovered (Fig. 7B,C). This indicates that not only are  $\text{Ca}^{2+}$  channels associated with dendritic spikes but that inhibition dominates excitation in blocking  $\text{Ca}^{2+}$  regenerative events using extracellular stimuli, as in L5 pyramidal cells (Pérez-Garci et al., 2006).

We took advantage of the fact that AP trains of suprathreshold frequency evoke dendritic electrogenesis equivalent to dendritic spikes to further explore the inhibition of dendritic regenerative events (and dendritic calcium influx) by GABAergic transmission. As in Figure 7, an extracellular electrode placed in L1 was used to generate a compound EPSP/IPSP using five pulses at 200 Hz. In addition, a train of bAPs above the CF was generated at various delays by current injection through the somatic patch electrode (Fig. 8A). We then analyzed distal calcium transients, measured near the principal bifurcation, as well as the ADP after the last AP in the somatic recording as a function of the delay between synaptic stimulation and the AP train. We found that dendritic electrogenesis and calcium influx were progressively blocked as the extracellular stimulus got closer in time to the AP train (Fig. 8B). This block was apparent even for long delays of  $>300$  ms. Only at 400 ms delay between stimuli did the calcium transients and ADP reach their control amplitudes (Fig. 8C,D). Suppression of the dendritic spike was attributable to the IPSPs because addition of antagonists of GABAergic transmission to the perfusate prevented blockade of the dendritic spike by the stimulus to L1 (data not shown).

## Discussion

The results presented in this paper complement the findings of Waters et al. (2003) in which we demonstrated that many of the properties of L2/3 pyramidal neurons are similar *in vitro* and *in vivo*. Here we investigated in more detail the regenerative properties of L2/3 pyramidal cell dendrites using dual recordings *in vitro* (which we were unable to achieve *in vivo*). We found that L2/3 pyramidal neurons share many features with L5 pyramidal neurons but also have distinct features that will influence their role in the cortical network. Most prominent among the similarities is the existence of a spike initiation zone in the distal apical dendrite, which acts as a second functional compartment and allows L2/3 pyramidal neurons to associate distal apical input with AP activity. In addition, we found that an inhibition blocks this dendritic activity with the same long timescale found in L5 pyramidal neurons (Larkum et al., 1999b; Pérez-Garci et al., 2006).

The most noticeable difference to L5 neocortical pyramidal neurons is that L2/3 dendrites support only brief dendritic spikes, not plateau potentials. Consequently, dendritic spikes facilitated by backpropagating APs caused only a single additional AP, not bursts of three or more APs. The lower capability of L2/3 neurons to generate AP bursts is seen *in vivo* (de Kock et al., 2007) and has consequences for the function of L5 and L2/3 pyramidal neurons in cortical networks (Lisman, 1997; Williams and Stuart, 1999). Another notable difference is the near absence of  $I_h$  in L2/3 neurons, which in L5 pyramidal neurons shunts the tuft dendrite (Williams and Stuart, 2000; Berger et al., 2001).

## Common features of L2/3 and other pyramidal neurons

### Dendritic spikes

We found that input to the distal apical dendrite in L2/3 cells can initiate a dendritic spike involving both  $\text{Na}^+$  and  $\text{Ca}^{2+}$  currents. Dendritic spikes in L2/3 pyramidal neurons resemble dendritic  $\text{Na}^+$  spikes in hippocampal CA1 neurons (Golding and Spruston, 1998; Gasparini et al., 2004) and fast dendritic spikes in L5 neocortical pyramidal neurons that were evoked by short current injection (Larkum et al., 2001). Nonetheless, dendritic spikes in L2/3 neurons were associated with large dendritic  $\text{Ca}^{2+}$  influx, demonstrating activation of dendritic  $\text{Ca}^{2+}$  channels. The likelihood of eliciting dendritic spikes was highest when stimulating the upper 60% of the apical dendrite. This effectively means that inputs to the apical dendrite in L1 and upper L2 may cause dendritic spikes. Interestingly, despite the fact that the tuft dendrite of L2/3 pyramidal neurons is substantially closer to the soma than in L5 neurons, isolated dendritic potentials (i.e., without a somatic AP) were more common in L2/3 neurons (cf. Zhu, 2000). This difference is probably attributable to the small diameter of the L2/3 dendrite, implying a higher axial resistance (Larkman et al., 1992), and the fact that the dendritic spike is much briefer than in L5 pyramidal neurons.

### Associative properties

The threshold for dendritic spike generation was high, but near-coincident bAPs reduced this threshold, much as in L5 pyramidal neurons (Larkum et al., 1999b). Because the tuft dendrites of L2/3 and L5 neurons overlap in L1, it seems likely that they would receive similar feedback inputs from higher cortical areas (Rockland and Pandya, 1979; Felleman and Van Essen, 1991; Lavenex and Amaral, 2000) and nonspecific thalamic inputs (Diamond, 1995). The associative properties of the apical dendrites are probably not as potent in L2/3 pyramidal neurons because (1) the threshold reduction by AP activity is smaller compared with L5 pyramidal neurons and (2) the dendritic spike produces at most one extra somatic AP, not the full-blown burst of three or more APs seen in L5 neurons (Larkum et al., 1999b). At the level of a cortical circuit, this lower efficacy in terms of additional single-cell output activity could be counterbalanced, however, by the greater number of L2/3 than of L5 pyramidal neurons (Peters et al., 1985).

### Critical frequency and inhibition

High-frequency trains of bAPs evoked supralinear  $\text{Ca}^{2+}$  influx into the distal apical dendrite (Waters et al., 2003). The critical frequency was slightly higher compared with L5 neurons (128 vs ~100 Hz) (Larkum et al., 1999a). In addition, the transition from subcritical to suprathreshold responses occurred over a greater range of frequencies. Nonetheless, the same criterion for defining the critical frequency was retained, namely, the turning point of the sigmoidal fit to the ADP versus frequency curve. Our mea-

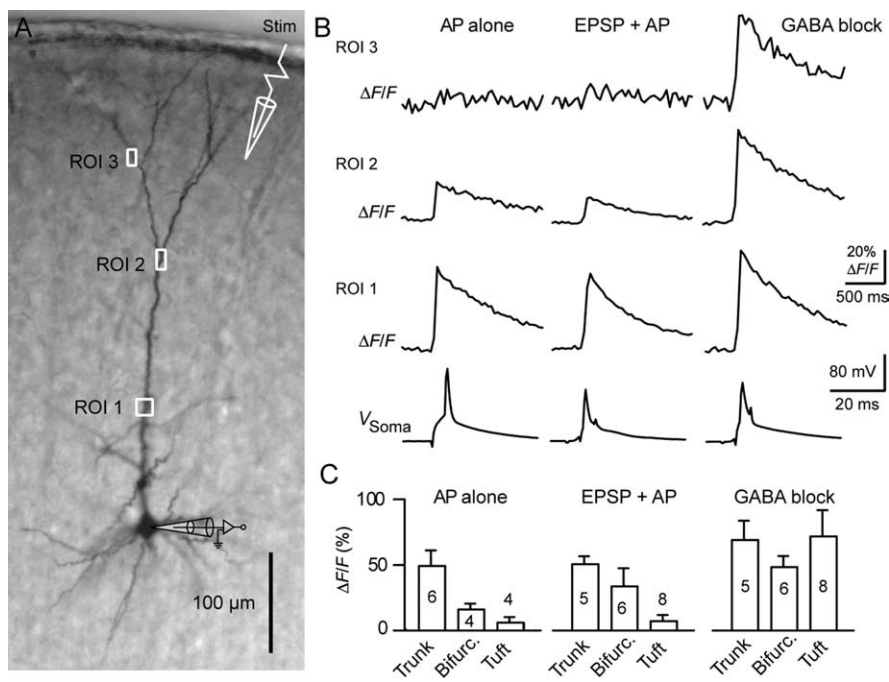


**Figure 7.** Synaptically evoked calcium influx into the apical dendritic tuft. **A**, Biocytin-filled L2/3 pyramidal neuron showing the locations of three ROIs at which calcium transients were measured. An extracellular electrode was placed in L1 to synaptically induce a compound EPSP. Single bAPs were elicited by brief current injections through the somatic pipette. Regions of interest correspond to the proximal apical dendrite (ROI 1), the main bifurcation (ROI 2), and the dendritic tuft (ROI 3). **B**, Calcium transients measured at the different locations indicated in **A**. Left column, A single AP caused very little calcium influx in the tuft. Middle column, Under control conditions, an extracellularly evoked EPSP that coincided with a bAP ( $\Delta t$  of 10 ms) did not cause a large  $[\text{Ca}^{2+}]_i$  increase in the tuft region. Right column, With the addition of  $2.5 \mu\text{M}$  bicuculline and  $1 \mu\text{M}$  CGP 55845 to the bath solution to block GABAergic transmission, coincidence of EPSP and AP evoked large  $[\text{Ca}^{2+}]_i$  transients in the distal tuft region and at all locations along the apical dendrite. **C**, Average amplitudes of calcium transients for the three stimulation paradigms one AP alone (left), EPSP plus AP (middle), and EPSP plus AP during block of GABAergic transmission (right). Calcium signals were grouped according to the location of the ROIs on the proximal apical dendrite (Trunk), the main bifurcation (Bifurc.), or dendritic tuft (Tuft). Numbers in the bars represent the number of cells for each condition.

surements were done in a large population sample by exploiting the finding that the somatic ADP robustly reflects dendritic excitation. Notably, the dendritic calcium signal amplitude observed above the critical frequency was the same as for a dendritic spike evoked by direct dendritic depolarization. This indicates that, in both cases, a regenerative dendritic event is triggered.

The  $\text{Ca}^{2+}$  influx that occurs during either a dendritic spike or a suprathreshold frequency train of bAPs can be blocked by extracellularly evoked inhibition as in L5 pyramidal neurons (Larkum et al., 1999a,b). Furthermore, the prolonged time course of this inhibition is identical to that in L5 neurons (Pérez-García et al., 2006), which suggests that the underlying mechanisms are the same, presumably involving metabotropic action of GABA receptors on dendritic  $\text{Ca}^{2+}$  channels (Kavalali et al., 1997). The specificity of this inhibitory action on dendritic  $\text{Ca}^{2+}$  activity implies that it is of functional importance for cortical processing. We suggest that this mechanism is important in preventing associations between feedback and feedforward pathways via pyramidal neurons. It should also prevent  $\text{Ca}^{2+}$ -dependent synaptic plasticity occurring in the distal tuft under certain conditions.

## Distinct features of L2/3 pyramidal cells

### Firing properties

The firing properties of L2/3 pyramidal neurons in response to injection of long depolarizing current steps at the soma were similar to those reported previously (Mason and Larkman, 1990),

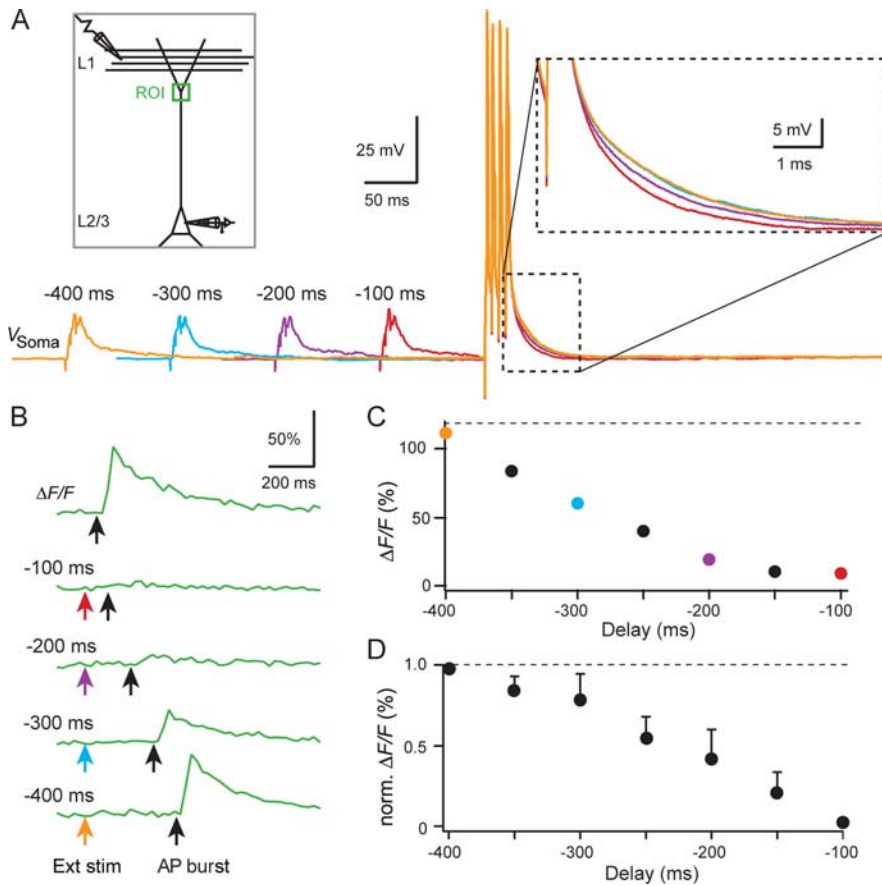


**Figure 8.** Long-lasting inhibition of dendritic calcium influx evoked by high-frequency AP trains. **A**, Four traces from an L2/3 pyramidal neuron. A train of four APs was generated at a frequency above the CF (at 150 Hz) with the somatic electrode. An extracellular stimulating electrode placed in L1 (500  $\mu\text{m}$  lateral to the cell) was used to evoke a compound EPSP/IPSP with five pulses at 200 Hz (inset shows experimental configuration). The extracellular stimuli preceded the four somatic APs by 100 ms (red trace), 200 ms (pink trace), 300 ms (blue trace), and 400 ms (orange trace). At 100 ms before the four somatic APs (red trace), the falling phase of the last AP was most attenuated (inset with dotted border). **B**, Calcium transients measured at the branch point in the distal dendrite without extracellular stimulus (top trace) and for each of the four recordings shown in **A** (bottom traces). Note that the  $[\text{Ca}^{2+}]_i$  increase in this region of the cell is blocked by extracellular stimuli applied  $<400$  ms before the AP burst. The colored arrows indicate the onset of the extracellular stimulus trains and the black arrows the onset of the AP train. **C**, Peak  $\Delta F/F$  values for the calcium transients shown in **B**, plotted as a function of the delay between the extracellular stimulus and the AP train. The dotted line indicates the change in fluorescence recorded with no extracellular stimulus. **D**, Averaged normalized  $\Delta F/F$  values as in **C** for three cells.  $\Delta F/F$  values were normalized to the peak fluorescence change recorded with no extracellular stimulation.

showing regular spiking with spike frequency adaptation. Unlike in both L5 and CA1 pyramidal neurons (Spruston et al., 1995; Stuart et al., 1997; Larkum et al., 2001), there was almost no spike amplitude adaptation in a train of backpropagating APs at any distance from the soma. In L5 pyramidal neurons, long depolarizing dendritic current injection evokes pronounced repetitive burst firing characteristic of intrinsically bursting neurons (Connors and Gutnick, 1990; Larkum and Zhu, 2002), even when the same current at the soma evokes a regular spiking pattern. Our findings here indicate that L2/3 pyramidal neurons of the somatosensory cortex in rats do not respond with long bursts to dendritic current injection. We never saw the fast rhythmic bursting or “chattering” L2/3 neurons seen in cat visual cortex *in vivo* with sharp electrodes (Gray and McCormick, 1996; Nowak et al., 2003) and in L2/3 of ferret cortex (Brumberg et al., 2000). Brumberg et al. (2000) showed that repetitive bursting in ferret L2/3 pyramidal neurons depends critically on the age ( $>4$  months) and extracellular calcium concentration ( $\leq 1.2$  mM). It is thus possible that the same constraints apply to rat cortex, which might explain the absence of such cells in this study.

## Sag

The input resistance showed an increasing relationship as a function of distance from the soma, which is different from L5 pyramidal neurons of the same age (Zhu, 2000). In L5 neurons, dendritic  $I_h$  has a counterbalancing role for input resistance (Berger et al., 2001) and leads to even more pronounced sag in the distal tuft region (Zhu, 2000; Williams and Stuart, 2000; Berger et al., 2001). We were therefore interested to test for dendritic sag with direct dendritic current injection. Although the slight sag in L2/3 pyramidal neurons indicated that some  $I_h$  current is present, it is far less pronounced than in L5 pyramidal neurons (Zhu, 2000) and does not affect the dendrite more than the cell body. Because  $I_h$  can reduce the amplitude and time window of summation of synaptic input (Williams and Stuart, 2002; Berger et al., 2003), the relative absence of  $I_h$  in L2/3 neurons suggests that the timing for association of top-down and bottom-up inputs might be different. Although the optimal separation of bAP and dendritic input appeared to be slightly longer (5–10 ms) than in L5 pyramidal neurons (Larkum et al., 1999b), this question will require a separate study.

## Conclusion

In conclusion, we found that L2/3 pyramidal neurons can generate dendritic spikes that are accompanied by large  $\text{Ca}^{2+}$  influx. L2/3 neurons thus can associate feedforward and feedback inputs arriving at the proximal and distal regions of the neuron. However, the dendritic  $\text{Ca}^{2+}$  influx can be prevented for a prolonged period of time by inhibition. Although these properties are similar to those of L5, the tuft dendrites of L2/3 neurons appear less coupled to the soma compared with L5 tufts. The associa-

tive properties demonstrated here will have consequences for the function of L2/3 pyramidal neurons in cortical microunits.

## References

- Agmon-Snir H, Segev I (1993) Signal delay and input synchronization in passive dendritic structures. *J Neurophysiol* 70:2066–2085.
- Amitai Y, Friedman A, Connors BW, Gutnick MJ (1993) Regenerative activity in apical dendrites of pyramidal cells in neocortex. *Cereb Cortex* 3:26–38.
- Berger T, Larkum ME, Lüscher HR (2001) High  $I_h$  channel density in the distal apical dendrite of layer V pyramidal cells increases bidirectional attenuation of EPSPs. *J Neurophysiol* 85:855–868.
- Berger T, Senn W, Lüscher HR (2003) Hyperpolarization-activated current  $I_h$  disconnects somatic and dendritic spike initiation zones in layer V pyramidal neurons. *J Neurophysiol* 90:2428–2437.
- Binzegger T, Douglas RJ, Martin KA (2004) A quantitative map of the circuit of cat primary visual cortex. *J Neurosci* 24:8441–8453.
- Brumberg JC, Nowak LG, McCormick DA (2000) Ionic mechanisms underlying repetitive high-frequency burst firing in supragranular cortical neurons. *J Neurosci* 20:4829–4843.
- Connors BW, Gutnick MJ (1990) Intrinsic firing patterns of diverse neocortical neurons. *Trends Neurosci* 13:99–104.

- de Kock CP, Bruno RM, Spors H, Sakmann B (2007) Layer- and cell type-specific suprathreshold stimulus representation in rat primary somatosensory cortex. *J Physiol (Lond)* 15:139–154.
- Diamond ME (1995) Somatosensory thalamus of the rat. In: *Cerebral cortex: the barrel cortex of rodents* (Jones EG, Diamond ME, eds), pp 189–220. New York: Plenum.
- Felleman DJ, Van Essen DC (1991) Distributed hierarchical processing in the primate cerebral cortex. *Cereb Cortex* 1:1–47.
- Gasparini S, Migliore M, Magee JC (2004) On the initiation and propagation of dendritic spikes in CA1 pyramidal neurons. *J Neurosci* 24:11046–11056.
- Golding NL, Spruston N (1998) Dendritic sodium spikes are variable triggers of axonal action potentials in hippocampal CA1 pyramidal neurons. *Neuron* 21:1189–1200.
- Gray CM, McCormick DA (1996) Chattering cells: superficial pyramidal neurons contributing to the generation of synchronous oscillations in the visual cortex. *Science* 274:109–113.
- Grossberg S, Raizada RD (2000) Contrast-sensitive perceptual grouping and object-based attention in the laminar circuits of primary visual cortex. *Vision Res* 40:1413–1432.
- Gulledge AT, Kampa BM, Stuart GJ (2005) Synaptic integration in dendritic trees. *J Neurobiol* 64:75–90.
- Helmchen F (2005) Calibration of fluorescent calcium indicators. In: *Imaging neurons: a laboratory manual* (Yuste R, Konnerth A, eds), pp 253–263. New York: Cold Spring Harbor Laboratory.
- Kavalali ET, Zhuo M, Bito H, Tsien RW (1997) Dendritic  $Ca^{2+}$  channels characterized by recordings from isolated hippocampal dendritic segments. *Neuron* 18:651–663.
- Kim HG, Connors BW (1993) Apical dendrites of the neocortex: correlation between sodium- and calcium-dependent spiking and pyramidal cell morphology. *J Neurosci* 13:5301–5311.
- Larkman AU, Major G, Stratford KJ, Jack JJ (1992) Dendritic morphology of pyramidal neurons of the visual cortex of the rat. IV. Electrical geometry. *J Comp Neurol* 323:137–152.
- Larkum ME, Zhu JJ (2002) Signaling of layer 1 and whisker-evoked  $Ca^{2+}$  and  $Na^{+}$  action potentials in distal and terminal dendrites of rat neocortical pyramidal neurons *in vitro* and *in vivo*. *J Neurosci* 22:6991–7005.
- Larkum ME, Kaiser KM, Sakmann B (1999a) Calcium electrogenesis in distal apical dendrites of layer 5 pyramidal cells at a critical frequency of back-propagating action potentials. *Proc Natl Acad Sci USA* 96:14600–14604.
- Larkum ME, Zhu JJ, Sakmann B (1999b) A new cellular mechanism for coupling inputs arriving at different cortical layers. *Nature* 398:338–341.
- Larkum ME, Zhu JJ, Sakmann B (2001) Dendritic mechanisms underlying the coupling of the dendritic with the axonal action potential initiation zone of adult rat layer 5 pyramidal neurons. *J Physiol (Lond)* 533:447–466.
- Larkum ME, Senn W, Lüscher H-R (2004) Top-down dendritic input increases the gain of layer 5 pyramidal neurons. *Cereb Cortex* 14:1059–1070.
- Lavenex P, Amaral DG (2000) Hippocampal-neocortical interaction: a hierarchy of associativity. *Hippocampus* 10:420–430.
- Lisman JE (1997) Bursts as a unit of neural information: making unreliable synapses reliable. *Trends Neurosci* 20:38–43.
- Lübke J, Roth A, Feldmeyer D, Sakmann B (2003) Morphometric analysis of the columnar innervation domain of neurons connecting layer 4 and layer 2/3 of juvenile rat barrel cortex. *Cereb Cortex* 13:1051–1063.
- Mason A, Larkman A (1990) Correlations between morphology and electrophysiology of pyramidal neurons in slices of rat visual cortex. II. Electrophysiology. *J Neurosci* 10:1415–1428.
- Nowak LG, Azouz R, Sanchez-Vives MV, Gray CM, McCormick DA (2003) Electrophysiological classes of cat primary visual cortical neurons *in vivo* as revealed by quantitative analyses. *J Neurophysiol* 89:1541–1566.
- Pérez-Garci E, Gassmann M, Bettler B, Larkum ME (2006) The GABA(B1b) isoform mediates long-lasting inhibition of dendritic  $Ca^{2+}$  spikes in layer 5 somatosensory pyramidal neurons. *Neuron* 50:603–616.
- Peters A, Kara DA, Harriman KM (1985) The neuronal composition of area 17 of rat visual cortex. III. Numerical considerations. *J Comp Neurol* 238:263–274.
- Rockland KS, Pandya DN (1979) Laminar origins and terminations of cortical connections of the occipital lobe in the rhesus-monkey. *Brain Res* 179:3–20.
- Schiller J, Schiller Y, Stuart G, Sakmann B (1997) Calcium action potentials restricted to distal apical dendrites of rat neocortical pyramidal neurons. *J Physiol (Lond)* 505:605–616.
- Schwindt P, Crill W (1999) Mechanisms underlying burst and regular spiking evoked by dendritic depolarization in layer 5 cortical pyramidal neurons. *J Neurophysiol* 81:1341–1354.
- Spruston N, Schiller Y, Stuart G, Sakmann B (1995) Activity-dependent action-potential invasion and calcium influx into hippocampal CA1 dendrites. *Science* 268:297–300.
- Stuart G, Schiller J, Sakmann B (1997) Action potential initiation and propagation in rat neocortical pyramidal neurons. *J Physiol (Lond)* 505:617–632.
- Svoboda K, Helmchen F, Denk W, Tank DW (1999) Spread of dendritic excitation in layer 2/3 pyramidal neurons in rat barrel cortex *in vivo*. *Nat Neurosci* 2:65–73.
- Traub RD, Buhl EH, Gloveli T, Whittington MA (2003) Fast rhythmic bursting can be induced in layer 2/3 cortical neurons by enhancing persistent  $Na^{+}$  conductance or by blocking BK channels. *J Neurophysiol* 89:909–921.
- Walcott EC, Langdon RB (2001) Short-term plasticity of extrinsic excitatory inputs to neocortical layer 1. *Exp Brain Res* 136:143–151.
- Walcott EC, Langdon RB (2002) Synaptically driven spikes and long-term potentiation in neocortical layer 2/3. *Neuroscience* 112:815–826.
- Wang XJ (1999) Fast burst firing and short-term synaptic plasticity: a model of neocortical chattering neurons. *Neuroscience* 89:347–362.
- Waters J, Helmchen F (2004) Boosting of action potential backpropagation by neocortical network activity *in vivo*. *J Neurosci* 24:11127–11136.
- Waters J, Helmchen F (2006) Background synaptic activity is sparse in neocortex. *J Neurosci* 26:8267–8277.
- Waters J, Larkum M, Sakmann B, Helmchen F (2003) Supralinear  $Ca^{2+}$  influx into dendritic tufts of layer 2/3 neocortical pyramidal neurons *in vitro* and *in vivo*. *J Neurosci* 23:8558–8567.
- Williams SR, Stuart GJ (1999) Mechanisms and consequences of action potential burst firing in rat neocortical pyramidal neurons. *J Physiol (Lond)* 521:467–482.
- Williams SR, Stuart GJ (2000) Site independence of EPSP time course is mediated by dendritic I-h in neocortical pyramidal neurons. *J Neurophysiol* 83:3177–3182.
- Williams SR, Stuart GJ (2002) Dependence of EPSP efficacy on synapse location in neocortical pyramidal neurons. *Science* 295:1907–1910.
- Zador AM, Agmon-Snir H, Segev I (1995) The morphoelectronic transform: a graphical approach to dendritic function. *J Neurosci* 15:1669–1682.
- Zhu JJ (2000) Maturation of layer 5 neocortical pyramidal neurons: amplifying salient layer 1 and layer 4 inputs by  $Ca^{2+}$  action potentials in adult rat tuft dendrites. *J Physiol (Lond)* 526:571–587.
- Zilles K (1990) *Anatomy of the neocortex: cytoarchitecture and myeloarchitecture*. pp 77–113. Cambridge, MA: MIT.